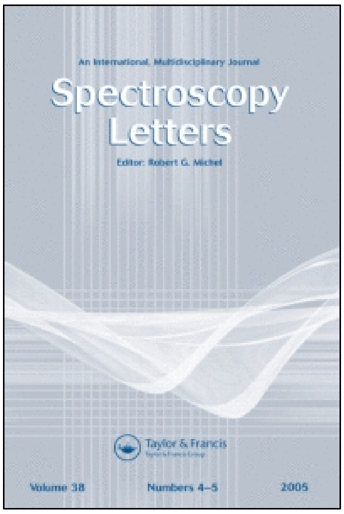

Spectroscopy Letters
Publication details, including instructions for authors and subscription information:
http://www.informaworld.com/smpp/title~content=t713597299

Microwave Frequency-Domain Spectroscopy of Complex Heterogeneous Nanocomposites: The Electromagnetic Functionality

Christian Brosseau[a]
[a] Laboratoire d'Electronique et Systèmes de Télécommunications, Université de Bretagne Occidentale, Brest, France

Online publication date: 22 June 2010

To cite this Article Brosseau, Christian(2008) 'Microwave Frequency-Domain Spectroscopy of Complex Heterogeneous Nanocomposites: The Electromagnetic Functionality', Spectroscopy Letters, 41: 6, 273 — 284
To link to this Article: DOI: 10.1080/00387010802286676
URL: http://dx.doi.org/10.1080/00387010802286676

Spectroscopy Letters, 41:273–284, 2008

ISSN: 0038-7010 print/1532-2289 online
DOI: 10.1080/00387010802286676

Microwave Frequency-Domain Spectroscopy of Complex Heterogeneous Nanocomposites: The Electromagnetic Functionality

Christian Brosseau
Laboratoire d'Electronique et Systèmes de Télécommunications, Université de Bretagne Occidentale, Brest, France

ABSTRACT We present systematic effective permeability measurements of nanostructured granular systems composed of magnetic (Ni) grains embedded in a nonmagnetic (ZnO) matrix using broadband microwave spectroscopy. Using the transmission/reflection waveguide method, the effective complex permeability was measured in the frequency range 0.01–10 GHz. From the data collected, it is found that a mean-field approach (effective medium approximation) is appropriate for understanding the permeability of composite materials characterized by submicrometer inclusion length scales. A systematic study of the room temperature effective permeability tensor of these composite samples is performed and provides a signature for the nonreciprocity of wave propagation in these nanostructures.

KEYWORDS effective magnetic permeability, microwave, nanocomposites

INTRODUCTION

Nanoscale magnetism and electromagnetism have been the subject of much research, both in fundamental studies and in technological applications. The topics range from magnetic-field sensing to magnetic recording heads, from DNA binding and magnetofection to biological imaging.[1–3] Recently, the conceptual tools and experimental methods developed in these studies have been applied with varying degrees of success to explore new types of nanostructured materials. As a result, there exist new opportunities to tailor the electromagnetic and magnetic properties through the choice of magnetic species and composition, potentially leading to novel structural forms, such as the core-shell nanostructures. These promising applications arise from their interesting physical properties such as superparamagnetism relaxation[4] and noncollinear (canted) spin structures.[5–7] Some of the envisioned magnetic and magnetoelectronic device applications using the nanophases are based on solid-state materials where the nanophases

Received July 6, 2007;
accepted November 28, 2007.

Address correspondence to Christian Brosseau, Laboratoire d'Electronique et Systèmes de Télécommunications, Université de Bretagne Occidentale, CS 93837, 6 avenue Le Gorgeu, 29238 Brest Cedex 3, France. E-mail: christian.brosseau@univ-brest.fr

are assembled into close-packed granular solids. They therefore offer the possibility of fabricating small devices being installed into larger systems. Miniaturization has many advantages including increased speed and sensitivity, reduced power consumption, and improvement in the spatial precision with which complex functions can be performed. Lightweight, small feature size, possibly biocompatible would in turn enable a range of applications, across many fields, e.g., biosensor arrays and high-frequency devices.[8] Such structures will not only possess a higher density of integrated circuits (ICs) but will also facilitate the use of quantum-information processing principles to enable an orders-of-magnitude increase in information processing capabilities.[9] These applications, however, will only gain market acceptance if they can be produced at a substantially lower cost than that of current available techniques. As a result, the current interest in magnetic nanomaterials is coupled with considerable effort aimed at developing new controllable fabrication routes as a low-cost technique compatible with monolithic microwave integrated circuits (MMICs).

Nanomaterials technology road map[10] calls for nondestructive and fast turnaround methods to measure the electromagnetic wave transport properties such as the permittivity and magnetic permeability. Microwave frequency-domain spectroscopy (GHz-FDS) has become an invaluable tool for the characterization of materials owing to the recent progress in instrumentation and experimental techniques. The issues and problems associated with microwave magnetic response of nanoscale structures are complex and varied and revolve around topics that are at the frontier of what is known in magnetism. In particular, the development of novel approaches to the characterization of nonreciprocal materials highlights the potential of GHz-FDS in studies of nanostructures. In order to become the material of choice for MMIC devices, nanomaterials need to demonstrate a level of performance much greater than the ferrite state of the art. Ferrites are important magnetic materials. Because of their large bandwidth, low electrical conductivity, low insertion loss, and frequency agility, ferrite devices have wide applications in technology, especially at high frequencies.[11, 12] Thick, highly oriented films of hexagonal ferrites (hexaferrites) having large uniaxial magnetocrystalline anisotropy are useful for planar nonreciprocal devices operating at GHz frequencies,[13] however, uses of these materials have been limited because of large microwave magnetic losses. With the continuing progress of IC technology, the requirement to increase the device density has led many to consider the use of nanophases and nanocomposites (NCs) for various aspects of nanofabrication. The current work was motivated by the question: Are they alternative materials within the broad class of NCs that offer improved performance (e.g., tunability) beyond that of ferrites for microwave applications?

Among the many types of nanostructured nanomaterials, NCs correspond with those that present at least one phase in nanoscale dimensions. Nanogranular materials are materials that consist of individual grains of the order several to hundreds of nanometers. Aggregates of nanoparticles are important in the context of magnetic phenomena as they serve as a bridge between the atomic limit and the bulk and can form a basis for understanding the emergence of magnetization as a function of size. The existing literature on the wave transport properties in NCs is not extensive although some interesting points have already been considered and investigated as it triggers a rich range of experimental behaviors that are appreciably different from those in the bulk. Reasons for this are the confinement of electrons in nanometric dimensions that gives rise to changes in the electronic distribution and thus in the optical, electromagnetic, transport (and so forth) properties and to the surface effects. Indeed, due to the large ratio of surface area to volume in nanosized objects, the behavior of surfaces and interfaces becomes a prominent factor controlling the physical and chemical properties of nanostructured materials. In fact, a particle with 1000 atoms has about 40% of them at the surface.[14] In addition the coupling of wave with structures much smaller than the wave's wavelength (typically, interaction lengths less than 100 nm) makes NCs interesting systems to charcaterize via effective-medium modeling.

In this context, current consensus is that the following questions have not been definitively answered: (1) How does a powder compact consisting of many grain boundaries behave magnetically, and how can the nanoparticles be densified into a bulk material while retaining the nanostructure of these particles? (2) How is the particle packing modified as the surface area to volume ratio increases (i.e., when the size of a particle decreases)? (3) How do material parameters, shape, size of magnetic structures, in addition to saturation magnetization, exchange stiffness, and anisotropy, affect their magnetic properties? One of the principal difficulties in answering these pressing questions pertains to the fact that the magnetic properties of nanostructures are strongly influenced by finite-size and surface effects. The electromagnetic and magnetic characterizations of these systems have put forward the controversial issue of distinguishing between the contributions coming from finite-size and surface effects. In addition, the electromagnetic characteristics will be affected by other features such as local strains, impurities, and so forth, that result from synthesis and processing. From the preponderance of the past results, the following conclusions can be drawn on item (1), Grain growth occurs at high temperature and results in coalescence of the particles and magnetic coupling of the ferromagnetic particles.[15,16] We note that whereas the magnetic properties of isolated single domain particles are well understood, it is not clear what effects magnetostatic interactions will have on assembly of nanophases. These interactions induce collective behavior between the particles and eventually give rise to complexities that cannot be explained by the Stoner–Wohlfarth theory (SW).[17] Regarding item (2), previous studies indicate that the packing of fine particles is affected by a set of factors, such as the actual particle size, its distribution, the particle shape, the particle friction, and its density.[18] Because van der Waals attractive forces and electrostatic interactions dominate over the gravity at the submicrometer scale, agglomerates and aggregates play a dominant role in several fields of nanotechnology.[19] Aggregates are formed by self-assembly of particles, which are bound to each other by strong, short-ranged noncovalent interactions. The number of atoms that participate in nano-aggregates controls the characteristics of these structures and may lead to a significant increase in magnetic moment. Regarding item (3), micromagnetic simulations and experimental results from numerous studies showed that these remanence-enhanced materials must have a grain size below 20 nm in order to exhibit good magnetic properties.[20] A set of recent studies has also indicated a variety of types of magnetic behavior originating from the symmetry and size of the nanostructures[21,22] and may be attributed to a competition between the exchange and magnetostatic interactions. However, the explanation of transport, item (1), is more complicated, for example, what precisely the damping mechanism really entails is still a controversial issue (see, e.g., Refs. 23–25). Optimization of magnetic materials with new functionalities requires a fundamental, quantitative understanding of the magnetization mechanisms in the presence of an induction field.

This work is structured as follows. The next section is devoted to a brief review of the different modeling approaches of the wave interaction with NCs. The following section takes up the subject of evaluating the effective magnetic permeability of NCs, with two purposes in mind. First, in order to characterize experimentally the material parameters, we need to know how to measure them. Our second purpose is to try to model the experimental data within effective medium analysis. The fourth section concludes the main text with a discussion of the implications for characterizing the wave transport in NCs, and the final section provides suggestions for future work that could significantly advance our knowledge of the electromagnetic properties of NCs.

MODELING OF THE WAVE INTERACTION WITH NANOCOMPOSITE MATERIALS

Because of their unique structure, which is characterized by a high surface-to-volume ratio, with a high proportion of atoms residing in the grain boundary regions, and a rather high density of crystals defects, nanocrystalline materials have extraordinary fundamental properties that could be exploited to make "next-generation" materials. Although many theoretical and experimental studies on nanosized grains were carried out on large assemblies of particles, many aspects of the static and dynamical magnetoelectronic properties of granular systems are not understood, impeding full exploitation of these systems. The search for new materials has been mainly empirical, as no predictive theory is currently known for the transport properties in nanostructures. However, over the years theoretical calculations have given some insight into the basic mechanisms, although the calculations concern idealized structures whereby the clusters are of essentially constant radius, uniformly distributed throughout the material, and with no interactions. While previous works concerned with experiments and modeling efforts of the material parameters of bulk composite materials exist, relatively few studies have been carried out on the physics of (artificially) nano- and mesostructured materials for which small separations among nanoparticles are connected to multipolar interactions between particles, together with local giant field electromagnetic fluctuations. Hence, there is a lack of fundamental understanding of the role of morphologic parameters on the electromagnetic properties. The availability of precise electromagnetic data in nanophases, usually defined as aggregates containing a number of constituent particles ranging from 10^2 to 10^7, provides a further link to bridge the gap between the micro and macro worlds. Unusual electronic properties with particle size, such as colossal magnetoresistivity, and superparamagnetism are of particular current interest in metal-based oxides. Among the various macroscopic physical properties, the relative permittivity (ε) and the diagonal and nondiagonal components of the relative magnetic permeability tensor (resp. μ and κ) are quite sensitive to the the atomic, electronic, and microscopic changes.[1] We have recently been studying these materials parameters in order to find additional systems showing correlations among their magnetic and electrical properties and mesostructure. We have found that modifying the anisotropic properties of permeability tensors subject to static magnetic field results in varying propagation behaviors.[26,27]

Given this background, it is clear that in order to obtain a complete and fundamental understanding of electromagnetic wave transport in granular nanophases, it is important to be able to study experimentally the tensorial nature of the materials parameters. Although it is a serious challenge to prepare well dispersed (uniform) NCs of various compositions, an even more difficult problem is the measurement of the material parameters. A search of the literature reveals that the current characterization techniques used to investigate electromagnetic properties of NCs are limited. Shortcomings and limitations of these methods have been known for some time, and many methods and types of apparatus have been devised partly to overcome these problems. To date, virtually all electromagnetic wave transport experiments on NCs are performed with the measurements of scalar permittivity and permeability using conventional techniques (e.g., coaxial line measurement, measurement of the transmission/reflection coefficients of an asymmetric microstrip transmission line). Only very recently, the tensorial nature of the effective material parameters has been addressed experimentally, with emphasis on the nonreciprocity issue.[26,28] Polder [17] was the first to theoretically approach the problem of the tensorial analysis of the permeability in a uniformly magnetized single-domain anisotropic magnetic particle. His study revealed that the permeability is described by a second-rank Hermitian tensor $\vec{\mu} = \begin{bmatrix} \mu & j\kappa & 0 \\ -j\kappa & \mu & 0 \\ 0 & 0 & 1 \end{bmatrix}$ in the coordinate system such that the external field is applied in the positive z direction, with $\mu = \mu' - j\mu''$ (resp. $\kappa = \kappa' - j\kappa''$) being the diagonal term (resp. off-diagonal term), and where the single prime (resp. double prime) denotes real (resp. imaginary) part. Over the past decade, the drive to establish broadband measurement methods for monitoring simultaneously ε, μ and κ has given considerable impetus to the development of sensitive microwave spectroscopies. Clearly, experiments aimed toward a "complete" electromagnetic characterization of the magnetic permeability tensor have become de rigueur in recent times. In this work, we use a nonreciprocal strip transmission line measurement cell. This makes it possible to clearly distinguish between the diagonal and off-diagonal components of the permeability tensor. Furthermore, it provides new insights into the drastic changes in magnetic properties for anisotropic materials subjected to an applied magnetic field.

Another aspect that deserves attention is the issue of mean-field (coarse-grained) modeling of the electromagnetic parameters in these assemblies of nanophases. In the quasistatic approximation (i.e., when the characteric lengths of the heterogeneities are very small compared with the wavelength of the electromagnetic radiation) theoretical studies based on the effective medium approximation (EMA) provide insight into the different mechanisms that contribute to the polarization and magnetization of composites.[29] This condition is fulfilled for the magnetic nanophases in our NCs. However, the pre-

TABLE 1 Selected Physical Properties of the Nanosized (N) and Microsized (M) Powders Investigated in This Study

Powder	ZnO (N)	ZnO (M)	Ni (N)	Ni (M)
Average particle size[a,b,c,d]	49 nm	1 μm	35 nm	3.5 μm
Powder color	White	White	Black	Gray
Specific surface area BET[a] ($m^2\ g^{-1}$)	22	22	15.6	15.6
Morphology[c]	Elongated	Elongated	Spherical	Spherical
Crystal phase[a,d]	Wurtzite	Wurtzite	Fm3m (225) Ccp	Fm3m (225) ccp
Density[a] ($g\ cm^{-1}$)	5.6	5.61	8.9	8.9

[a] From manufacturer product literature.
[b] Determined from specific surface area.
[c] Checked by transmission electron microscopy images.
[d] Checked by X-ray diffraction experiments.

diction of the material properties based on these theoretical studies is cumbersome because of the difficulty of directly measuring the surface and interface contributions to these mechanisms. Moreover, a comparison of the measured electromagnetic parameters versus composition and EMT reveals discrepancies, presumably due to the poor characterizations of the distribution of particle sizes, shapes, and defects that render the interpretation quite difficult. Viau et al.[30] argued that a coarse-grained approach is unable to fully represent the physics of NCs. Despite the reasonable arguments made by Viau et al.,[30] as well as that our own results[26–28,31,32] to date have supported their analysis, additional evidence for the failure of effective medium theories in nanocrystalline materials would be welcome. Moreover, we expect that order parameters different from these volumic parameters are needed for a proper description of surface/interface effects on the magnetic anisotropy and permeability. Great care must be taken when interpreting dynamical properties in magnetic environments containing multiple length scales, because these properties are governed by several interacting processes taking place simultaneously at different length scales. For dynamical simulations, the relevant length scales should be coupled.

MATERIALS AND METHODS

Materials

All the samples used in these experiments consist of mixtures of fine powders of neat Ni and ZnO with a stable epoxy resin widely used for low-temperature experiments (Scotchcast 265) and purchased from 3 M (Austin, TX). The ratio of the powders to the resin is in the range 9–17% by volume. The starting nanopowders were purchased from Nanophase Technologies Corp. (Burr Ridge, IL) and were used without further purification. For the purpose of comparison, another set of samples was fabricated that contains mixtures of microsized powders (purchased from Aldrich Chemicals), and these samples are denoted as type M to distinguish them from the mixtures of nanosized powders (denoted as type N samples). Inspection of Table 1 shows the average size of the particles for Ni and ZnO, respectively.

Several series of samples (Table 2) were fabricated using conventional powder pressing. The detailed fabrication procedure to achieve homogeneous composition of the samples has already been described in previous publications.[23,26,27,31] Room-temperature-pressed ZnO/Ni compacts were made under a pressure of $10^7\ Nm^{-2}$ for 2 min. For the coaxial line measurement, the typical dimensions of the sample that was fabricated as toroids (APC 7 standard) were inner diameter of 3.04 mm, outer diameter of 7 mm, and length of 2 to 4 mm. For the strip transmission line measurement, parallelepipedic samples were cut and polished on all six faces until they reach the typical dimensions (5 mm long, 5 mm wide, and 1.8 mm thick), with a mass near 2 g.

TABLE 2 Overview of NCs Compositions: f_X Denotes the Volume Fraction of the X Species, f_p is the Porosity of the Samples, and f_{resin} is the Volume Fraction of Resin

Material designation	f_{Ni}	f_{ZnO}	f_p	f_{resin}
nNiZ0	0.56	0	0.19	0.14
nNiZ1	0.49	0.08	0.28	0.15
nNiZ2	0.42	0.17	0.27	0.14
nNiZ3	0.38	0.21	0.26	0.15
nNiZ4	0.33	0.26	0.25	0.15

Compaction pressure for all composites was 10^7 Nm for 2 min.

The morphology and size of the starting powders were determined by transmission electron microscopy (TEM) using a 200-kV Jeol (Jeol-2010) apparatus and selected area diffraction. Cross-sectional bright-field TEM images indicate that Ni particles are homogeneous with nearly spherical shape.[31] The wurtzite-type ZnO particles were rod-shaped with an aspect ratio of about 3:1, which was determined from TEM micrographs. The phase purity was checked by x-ray powder diffraction (XRD) using monochromatic Cu $K\alpha$ radiation (Phillips, PW-1729), and the average crystallite sizes were determined from the line broadening of the reflections using the Scherrer analysis. The grain sizes determined from analysis of bright-field cross-sectional TEM images are consistent with the ones obtained from XRD.

Electromagnetic Measurements

Our experimental facilities offer the opportunity to probe simultaneously the effective complex permittivity $\varepsilon = \varepsilon' - j\varepsilon''$ and permeability $\mu = \mu' - j\mu''$ of the composite samples. We present our results relative to the permittivity and permeability of vacuum. Two kinds of measurements were done. On the one hand, the material parameters ε and μ were measured using the transmission/reflection method[33] for the broadband characterization of isotropic solid materials. This experimental technique is based on the measurement of the scattering parameters (S parameters) of a toroidal sample of the test material that has been machined in order that the geometrical dimensions fit well those of the coaxial line used (to avoid the presence of air gaps between the sample and the line walls). The method is based on a two-port device connected to an S-parameter test set driven and controlled by a network analyzer.[31,32] In this coaxial line measurement, the fundamental transverse electromagnetic mode is the only mode that propagates in the coaxial line. An error analysis indicates modest uncertainties in ε' ($<5\%$), ε'' ($<1\%$), μ' ($<3\%$), and μ'' ($<1\%$) for the data. A Hewlett Packard HP 8720B network analyzer setup is used to measure the S parameters of the cell containing the material under test over a wide range of frequencies (10 MHz to 10 GHz) with SOLT (short-open-load-thru) calibration. All the experimental data reported in this article were obtained at room temperature. On the other hand, the microwave measurements of the effective magnetic (relative) permeability tensor $\overleftrightarrow{\mu}$ were done using a strip transmission line measurement method. Relevant aspects of the experimental setup utilized in the current measurements were first described in 2002.[28] A major concern in this characterization method is to identify the nonreciprocal properties of the tested sample. For a macroscopically isotropic two-phase composite medium, off-diagonal elements of the magnetic permeability $\overleftrightarrow{\mu}$ are equal to zero. However, there should be nonzero off-diagonal elements in $\overleftrightarrow{\mu}$ for magnetically anisotropic materials, and the reciprocity is broken. A conventional electromagnet was used to transversely and uniformly magnetize the sample to be characterized. A Hewlett Packard HP 8720 A network analyzer setup is used to measure the S parameters of the cell containing the material under test. All permeability spectra were recorded at room temperature.

RESULTS AND DISCUSSION

Coaxial Line Measurement of the Magnetic Permeability

Representative frequency dependence curves of the real and imaginary parts of the relative effective permeability μ for type N ($f_{Ni} = 0.50$, $f_{ZnO} = 0.08$, $f_{epoxy} = 0.14$, and porosity $= 0.28$) and type M ($f_{Ni} = 0.50$, $f_{ZnO} = 0.20$, $f_{epoxy} = 0.17$, and porosity $= 0.13$) Ni/ZnO composite samples are plotted in Fig. 1a, b. Upon inspection of Fig. 1a and Fig. 1b, one can see the differences between the permeability of M samples and that of N samples. As can be seen from Fig.1a and b, μ' decreases to zero (with a concomitant broad peak of μ'' in the GHz region of frequency). Perhaps the most noteworthy feature is that whatever the volume fraction of Ni investigated (from 0 vol% to 69 vol %), M samples do not show absorbing properties in the microwave range. In order to gain a better understanding of how the composition affects the permeability, a set of experiments was conducted in which the volume fraction of Ni is varied, as illustrated in Fig. 2a, b. It is noticeable that the data in Fig. 2a, b corresponding with M and N samples at $f = 1$ GHz, have very different behaviors. In particular, Fig. 2a, b indicates that the $\mu'(f_{Ni})$ and $\mu''(f_{Ni})$ curves show substantial changes from M and N samples (e.g., μ' is enhanced by a factor of 5 and μ'' is

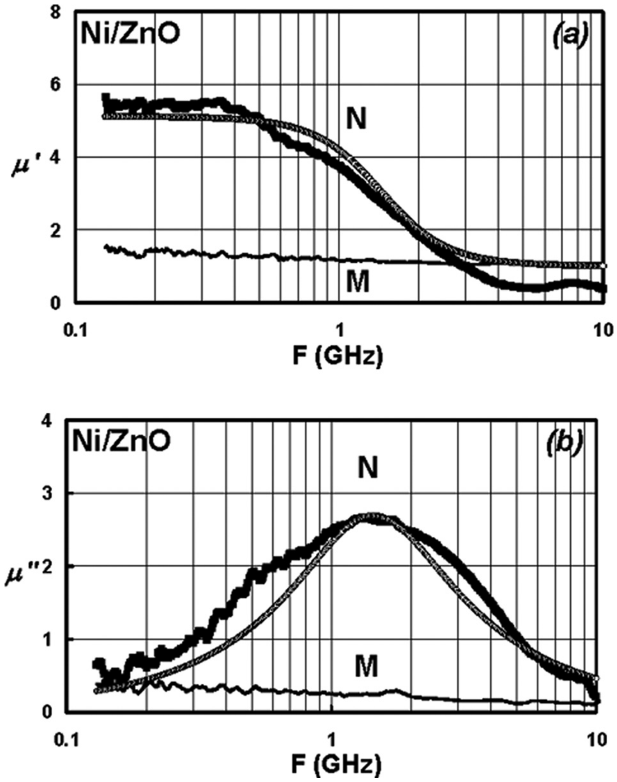

FIGURE 1 The frequency dependence of the relative permeability μ for micrometer-sized (M, thin curve) and nanometer-sized (N, thick curve) composite samples and a given value of the volume fraction of the magnetic phase. Room temperature. (a) Real part μ' of the permeability for Ni/ZnO composites. The composition is $f_{Ni} = 0.49$, $f_{ZnO} = 0.08$, $f_{epoxy} = 0.14$, and porosity = 0.28 for the type N sample (nNiZ1 in Table 2), and is $f_{Ni} = 0.50$, $f_{ZnO} = 0.20$, $f_{epoxy} = 0.17$, and porosity = 0.13 for the type M sample. The dashed line is a Lorentzian fit to the data. (b) Imaginary part μ'' of the permeability for Ni/ZnO composites. Same composition as in (a). The dashed line is a Lorentzian fit to the data.

enhanced by a factor of 15 for $f_{Ni} \approx 0.6$). It should also be noted that the resonance frequency F_0 is slightly increased as the percentage of Niis increased. One can see also from Fig. 3 that the resonance width at half height ΔF decreases significantly as the percentage of Ni is increased.

A related basic question is to examine the links with coarse-graining models based on the effective medium (mean-field) approximation. A basic assumption used in the theory of composites is that there exist length scales above which fluctuations at the microscopic level may be ignored. In this way, useful predictions of a granular material's bulk properties can be made with no references to its discrete nature. This major simplifying approximation is based on a self-consistent procedure in which a grain of one component is assumed to have a convenient

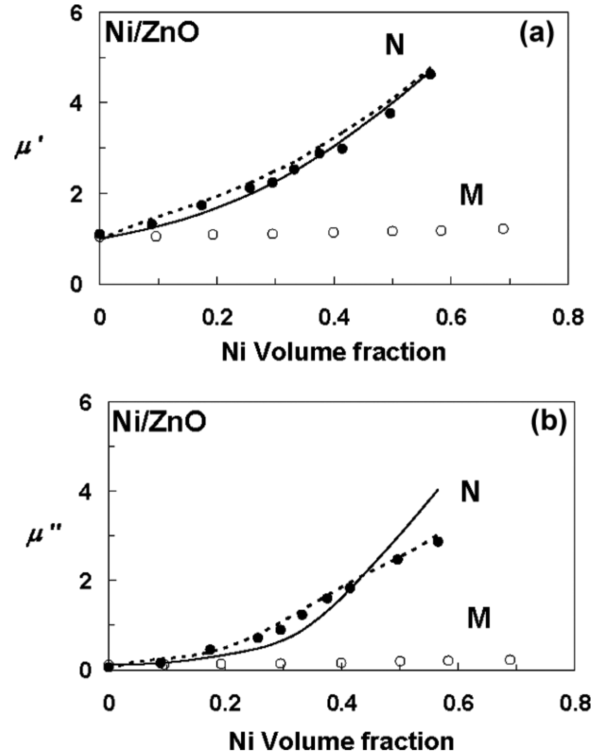

FIGURE 2 Variation of the relative permeability as a function of the volume fraction of the magnetic phase for M-type (open symbols) and N-type (filled symbols) composite samples at a given value of frequency, F = 1 GHz. Room temperature. The solid (resp. dashed) line is a fit to the data according to the Bruggeman (resp. McLachlan) model. (a) Real part μ' of the permeability for Ni/ZnO composites. (b) Imaginary part μ'' of the permeability for Ni/ZnO composites.

shape and to be embedded in an effective medium whose properties are determined self-consistently. Two prominent and standard approaches are to solve the Bruggeman or the McLachlan equations for the type of granular magnetic composites of interest in this article.[29] The results for type N

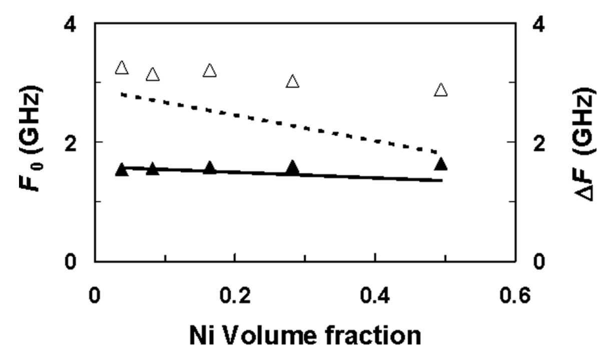

FIGURE 3 The resonance frequency F_0 (filled symbols) of Ni/ZnO nanocomposites as a function of the volume fraction of Ni. The resonance width ΔF (open symbols) as a function of the volume fraction of Ni. The solid (resp. dashed) line shows the calculated value of F_0 (resp. ΔF) using our modeling approach.

Ni/ZnO (Fig. 2a, b) are as one would expect: the increase of the magnetic content in the mixture results in an increase of μ' and μ''. The solid lines through the data in Fig. 2a–d are fits using the Bruggeman equation and provide an indication of some of the effects that control the effective permeability of nanocomposites. A permeability of unity was assigned to the pore regions, epoxy, and ZnO. This reproduces all features qualitatively, but quantitative agreement is poorer for μ''. It is to be noted that the extracted value of μ_{Ni} from fit of the μ versus f_{Ni} graphed in Fig. 1 (i.e., $\mu_{Ni}(1\,GHz) = 8\text{-}j6$), is consistent with previous studies of the zero-field magnetic resonance of composite materials composed of fine ferromagnetic Co_xNi_{1-x} and $Fe_z[Co_xNi_{1-x}]_{1-z}$ particles prepared by precipitation in 1,2-propanediol.[30] In like fashion, the McLachlan model would give $\mu_{Ni}(1\,GHz) = 5.8\text{-}j4.3$ for the Ni/ZnO nanocomposites (dashed line in Fig. 2a, b), to be compared with the value $\mu_{Ni}(1\,GHz) = 8\text{-}j6$ determined with the Bruggeman model. The percolation limit turns out to be 0.19 ± 0.01, slightly higher than the threshold of three-dimensional continuum percolation, that is, $\cong 0.17$.[29] Although this analysis provides a better fit to the experimental data, it did not offer any insight into the nature of the interaction between magnetic grains.

In Fig. 1a, b we present also a comparison of the μ' and μ'' experimental spectra with those derived from a simulation based on this modeling. We employ a Lorentzian line shape. Although there are systematic discrepancies to a certain extent, we note that the spectra of Fig. 1b exhibits the symmetry predicted by the Landau–Lifshitz–Gilbert equation (LLG).[17] Moreover, it can be concluded that the overall agreement of the spectral dependence of the observed μ' and μ'' with the LLG predictions is fairly good in view of the simple assumption made. To gain some idea of the trend on the resonance frequency F_o and the resonance width ΔF versus the Ni content, the predicted values are graphed in Fig. 3. Comparing the experimental features with the theoretical calculations for F_o and ΔF, we do observe a remarkable agreement for F_o. However, the observed ΔF are larger than the ΔF expected from the LLG modeling. It is also important to note that the value of α obtained ranged from 0.19 to 0.40. These agree with the values obtained from earlier calculations[26] for γ-Fe_2O_3/ZnO composites. One can independently obtain a value of α from FMR.[23] Although we have captured some of the resonance occuring in the nanocomposites, a deficiency of our approach is certainly that we fail to capture all of it. The

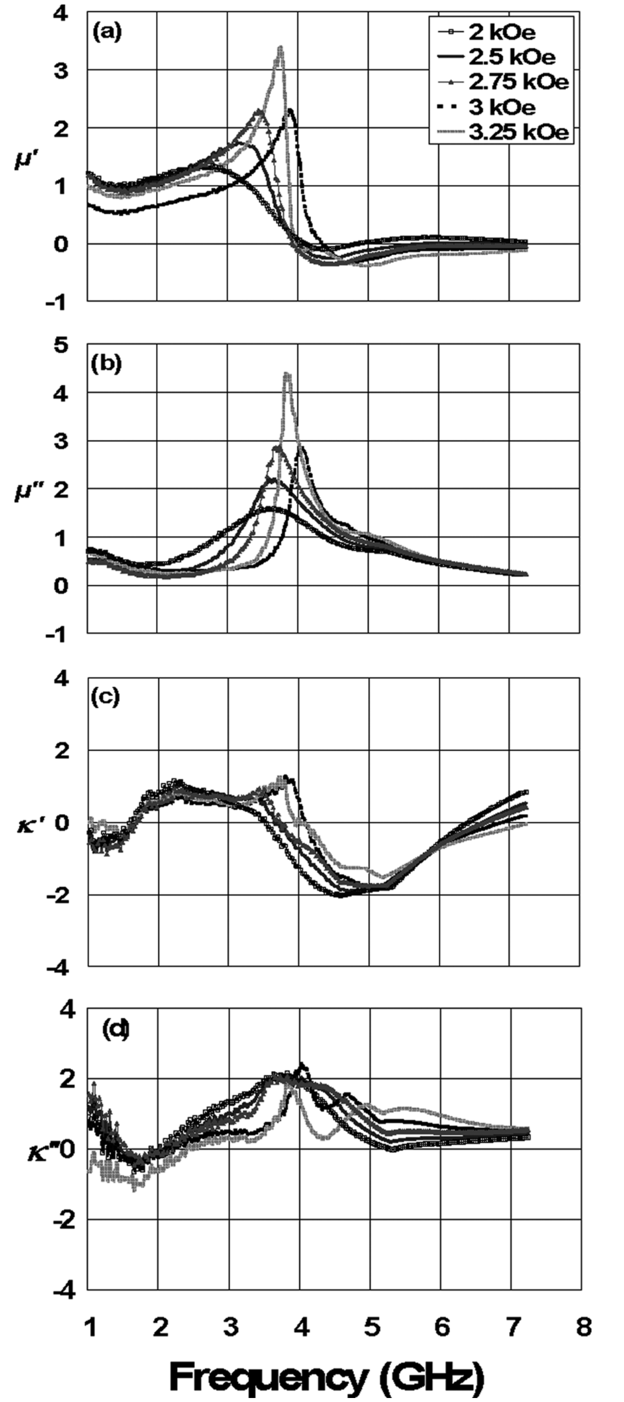

FIGURE 4 **Frequency dependence of the real part of the components μ and κ of the effective permeability tensor in N (nNiZ0) sample (see Table 2 for the corresponding concentrations of species) for magnetic field intensity varying between 2 and 3.25 kOe: (a) real part μ', (b) imaginary part μ'', (c) real part κ', (d) imaginary part κ''. The applied magnetic field is indicated in the inset. Room temperature.**

weakness of the modeling, however, is that it may be to simple due to the fact that we do not consider interface contributions, and this may be responsible for the broadening induced by the magnetic inhomogeneities to the gyroresonance peak. It should also be noted that the problem is not always well defined as the magnetic nanoparticles are polydisperse and the shape and size of the particles are not well-known.

Strip Transmission Line Measurement of the Magnetic Permeability

In our initial work[23,31,36] with the permeability tensor of NCs, we varied the volume fraction of the magnetic phase (γ-Fe_2O_3) in the nonmagnetic matrix. In Fig. 4, we present a set of representative spectra for the real and imaginary parts of the permeability tensor components at different values of the applied magnetic field for the neat Ni sample. From the panels of these figures, several observations can be made. The first remarkable result seen in Fig. 4 is that as the intensity of the magnetic field is increased the asymmetric peak positions of μ' and μ'' shift to higher frequency, except at 3.25 kOe for which the resonance frequency is less than that at 3 kOe. This observation remains valid for all Ni/ZnO NCs investigated. The second feature of note is the nonzero off-diagonal terms of the permeability tensor. A careful examination of Fig. 4c,d reveals that several bands appear in the κ' and κ'' spectra and that the maximum of μ'' is coincident with the corresponding maximum of κ''. Whereas the magnitude of μ' and κ' at 3.25 kOe is similar to the value obtained for saturated dense Y-Al ferrites[28], the corresponding values of the imaginary parts μ'' and κ'' are much smaller than those of the ferrite slab. The influence of the concentration of the magnetic phase on the spectra (the applied magnetic field is $H = 3$ kOe) is clearly seen in Fig. 5. Furthermore, a shift toward higher frequency in the peak position of the gyromagnetic resonance was observed as the volume fraction of Ni was decreased. Another aspect that deserves attention is the concomitant smaller width (e.g., we obtain a linewidth narrowing by a factor of 10 when f_{Ni} vary from 0.56 to 0.33). Figure 5a, b indicates that the μ' and μ'' curves show substantial changes as the Ni volume fraction is decreased (e.g., μ' and μ'' are enhanced by a factor of 2 when f_{Ni} changes from 0.56 to 0.33). Figure 5c, d indicates a strong magnetic anisotropy that is very sensitive to the magnetic phase concentration.

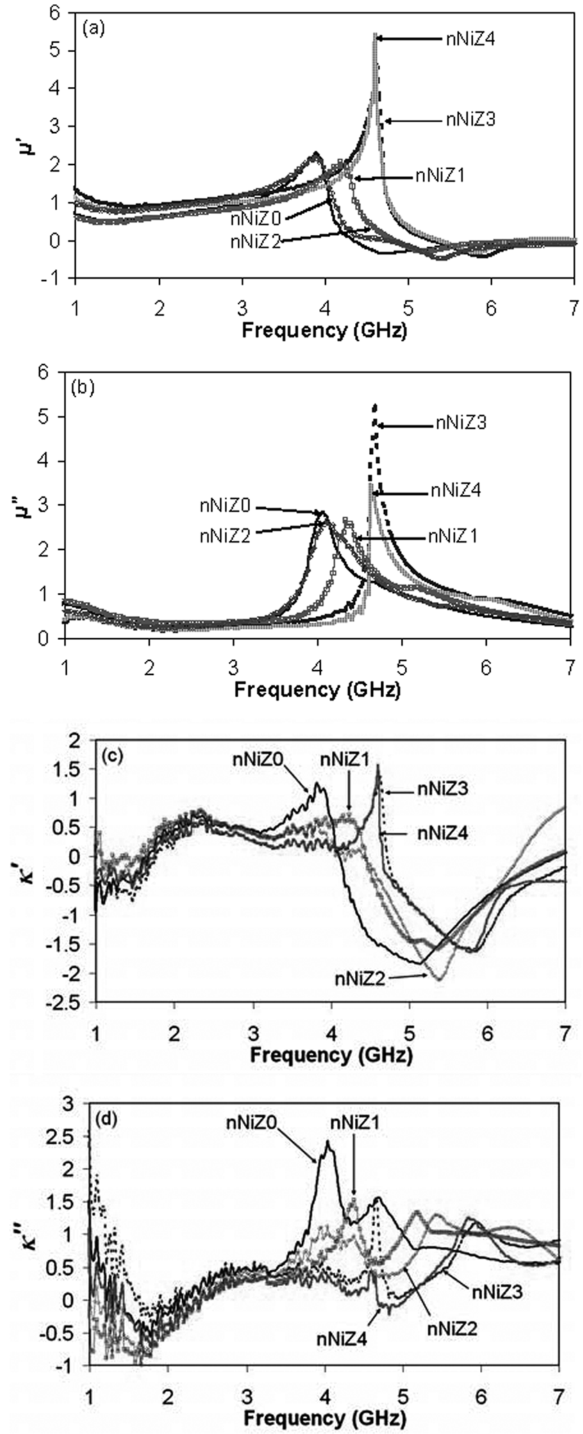

FIGURE 5 **(a) Frequency dependence of the real part of the components μ and κ of the effective permeability tensor in N samples Ni/ZnO: (a) real part μ', (b) imaginary part μ'', (c) real part κ', (d) imaginary part κ''. The applied magnetic field is $H = 3$ kOe. The sample designation (see Table 2 for the corresponding concentrations of species) is indicated in the figure. Room temperature.**

The above results suggest that a field-induced magnetic anisotropy can be achieved with Ni containing NCs. The data presented here may help to specify the nonreciprocal electromagnetic properties, embedded in the off-digaonal permeability tensor component, of magnetic nanophases. The field-induced magnetic anisotropy that is observed in Fig. 4 is relevant to the implementation of the nonreciprocal functionality employed in microwave isolators, phase shifters, and circulators. For example, this functionality would exhibit reduced insertion losses due to low values of μ'' and κ'' near the gyromagnetic resonance frequency, as exemplified by the permeability behavior of Ni/ZnO NCs shown in Fig. 4.

We further observe that the interest in the problem of magnetization mechanisms of nanophases was excited by the pioneering work of Aharoni[17] who recognized the role of grain size and composition in exchange modes. Recently, Mercier and co-workers[37] attempted to explore the influence of multiresonances. Interestingly, in a recent experimental study performed by us,[32] an overall agreement of the spectral dependence of the complex effective (scalar) permeability of Ni/ZnO NCs with the Landau–Lifshitz–Gilbert equation was found to be fairly good in view of the simple assumption. Analysis of the gyroresonance linewidths strongly suggested a large dispersion in the local field that presumably reflects the disordered physical nanostructure. Viau and co-workers[30] have analyzed the multiresonances observed in the effective (scalar) permeability of $Fe_{0.13}[Ni_{80}Co_{20}]_{0.87}$ systems in terms of nonuniform resonance modes resulting from the exchange energy contribution to the magnetization precession within the particles. These results are of intrinsic interest as well as being tied to more complex phenomena such as damping of spin motions in magnetic nanostructures for which the specific mechanisms are still debated.[1,23]

SUMMARY AND OUTLOOK

The above sections have described preparation methods and measurement results on the electromagnetic characteristics of NCs in the microwave range of frequencies. The initial goal of this investigation was to discover whether we could use the excellent performance reported for magnetic NCs as a guide to finding materials with improved characteristics compared with ferrites for microwave applications. In particular, we were interested in such important electromagnetic characteristics as tensorial effective magnetic permeability and effective permittivity, which are not as prominently featured in the literature.

A summary of the chief characteristics of the results of this experimental study is as follows. Taken together, the combined permeability tensor spectra measurements over a broad band of responses in the GHz regime show that magnetically structured granular systems composed of magnetic grains embedded in a nonmagnetic matrix can have very different behaviors depending on their constituents. It is found that mixing Ni nanoparticles with ZnO nanoparticles results in a smaller linewidth of the gyromagnetic resonance and an increased coercivity compared with a sample consisting solely of Ni nanoparticles.[27] With the current work and related recent studies, an extensive body of experimental data on the microwave magnetic response of nanoscale structures is now available.

Granular materials persist at the forefront of contemporary research. With the enormous number of conventional magnetic materials available to technology as the outcome of a century's progress, it is legitimate to ask what fundamentally original features the magnetodielectric nanostructured materials introduce in the field.[38] In our view there are three. First, and by no means last, is the issue of processing. Like other artificially structured solids, granular NCs contain intricate structure on the nanometer scale and extra degrees of freedom with which the physical properties can be manipulated to achieve tailored materials for applications and for exploration of physical phenomena. Improving the magnetic properties of nanopowder compacts is to make the exchange coupling between neighboring magnetic aggregates dominate the demagnetizing and magnetocrystalline anisotropy energies in the material. Second, these materials may facilitate the conversion between energies stored in magnetic and electric fields. However, and this is the third point, depending on the structural details, the local (residual) stress can also adversely affect other properties crucial to device performance, such as mechanical strength and aging. Therefore, the control of stress-induced strain is key to optimizing the processing conditions for implementation in the future microwave tunable devices to increase the speed of performance, reduce the dimensions, consume less power, and provide novel modes of operation in comparison with conventional counterparts (e.g., ferrites).

We emphasize in closing that the recent considerable attention in the research community in metal oxides nanophases (e.g., magneto-electric multiferroic $BaTiO_3$-$CoFe_2O_4$ nanostructures[39]) has revealed a range of interesting and intriguing properties that offer great promise for the design of materials with user-defined properties. The coexistence of both magnetic and ferroelectric orders raises the possibility of a subtle interplay between the electric polarization and magnetization mechanisms.[40, 41] The multidimensional nature of the interactions between the composition, process parameters, and end-use conditions of functional materials provides tremendous prospects for high-throughput nanomaterials research. It is of interest to explore further the electromagnetic response of these sophisticated materials as they are promising candidates for planar nonreciprocal devices operating at microwave wavelengths. It has been argued[1] that the years ahead may see magnetic nanometer-sized structures play a major role for application in magnetoelectronics. Whatever lies ahead down the road for granular magnetic NCs, the journey promises to be a particularly challenging and interesting one.

ACKNOWLEDGMENTS

The article is a much belated revision of lecture notes I provided for the Rencontre Internationale de Spectroscopie et d'Optique (RISO 2007) held in June 2007 at Kénitra (Morocco). Many colleagues have helped me to understand the issues covered in this topical review, and I thank particularly S. Mallégol, P. Quéffelec, and J Ben Youssef for many useful discussions and A.-M. Konn, F. Michaud, D. Rozuel, G. Sinquin, and P. Talbot for their technical assistance. The Laboratoire d'Electronique et Systèmes de Télécommunications is Unité Mixte de Recherche CNRS 6165.

REFERENCES

1. Nalwa, H. R., Ed. *Encyclopedia of Nanoscience and Nanotechnology*; American Scientific: New York, 2004; 10000.
2. Wolf, E. L. *Nanophysics and Nanotechnology*; Wiley-VCH: Weinheim, 2004; 187.
3. Cao, G. *Nanostructures and Nanomaterials*; Imperial College Press: London, 2004; 433.
4. Dormann, J. L.; Fiorani, D.; Tronc, E. Magnetic relaxation in fine-particle systems. In *Advances in Chemical Physics*; Prigogine, I.; Rice, S. A., Eds.; Wiley: New York, 1997, Vol. XCVIII; 283–494.
5. Coey, J. M. D. Non-collinear spin arrangement in ultrafine ferrimagnetic crystallites. Phys. Rev. Lett. **1971**, *27*(17), 1140–1143.
6. Morrish, A. H.; Haneda, K. Surface magnetic properties of fine particles. J. Magnetism Magnetic Mater. **1983**, *35*(1–3), 105–113.
7. Tronc, E.; Ezzir, A.; Cherkaoui, R.; Chanéc, C.; Noguès, M.; Kachkachi, H.; Fiorani, D.; Testa, A. M.; Grenèche, J. M.; Jolivet, J. P. Surface-related properties of γ-Fe_2O_3 nanoparticles. J. Magnetism Magnetic Mater. **2000**, *221*(1–2), 63–79.
8. Piqué, A.; Chrisey, D. B.; Fitz-Gerald, J. M.; McGill, R. A.; Auyeung, R. C. Y.; Wu, H. D.; Lakeou, S.; Nguyen, V.; Chung, R.; Duignan, M. Direct writing of electronic and sensor materials using a laser transfer technique. J. Mater. Res. **2000**, *15*(9), 1872–1875.
9. Crawley, D.; Nikolic, K.; Rorshaw, M. *3-D Nanoelectronic Computer Architecture and Implementation*; Taylor & Francis/CRC Press: London, 2004; 282.
10. *Chemical Industry R&D Roadmap for Nanomaterials By Design: From Fundamentals to Function*; Chemical Industry Vision 2020 Technology Partnership, Baltimore, MD, 2003; http://www.chemicalvision2020.org/nanomaterialsroadmap.html
11. Brabers, V. A. M. Progress in spinel ferrite research. In *Handbook of Magnetic Materials*, Vol. 8; Buschow, K. H. W., Ed.; Elsevier Science: New York, 1995; 65.
12. Valenzuela, R. *Magnetic Ceramics*; Cambridge University Press: Cambridge, 1994; 295.
13. Vittoria, C. Ferrite uses at millimeter wavelengths. J. Magnetism Magnetic Mater. **1980**, *21*(2), 109–118.
14. Edelstein, A. S.; Cammarata, R. C.; Eds. *Nanomaterials: Synthesis, Properties and Applications*; Institute of Physics: Bristol, 1996; 369.
15. Watanabe, M.; Masumoto, T.; Ping, D. H.; Hono, K. Microstructure and magnetic properties of FePt–Al–O granular thin films. Appl. Phys. Lett. **2000**, *76*(26), 3971–3973.
16. Zeng, H.; Sun, S.; Vedanta, T. S.; Liu, J. P.; Wang, Z. L. Exchange-coupled FePt nanoparticle assembly. Appl. Phys. Lett. **2002**, *80*(14), 2583–2585.
17. Aharoni, A. *Introduction to the Theory of Ferromagnetism*; Oxford University Press: Oxford, 2001; 328.
18. Israelachvili, J. N. *Intermolecular & Surface Forces*; Academic: London, 1991; 600.
19. Kendall, K. Adhesion: molecules and mechanics. Science **1994**, *263*(5154), 1720–1725.
20. Schrefl, T.; Fidler, J.; Kronmuller, H. Remanence and coercivity in isotropic nanocrystalline permanent magnets. Phys. Rev. B **1994**, *49*(9), 6100–6110.
21. Cowburn, R. P.; Koltsov, D. K.; Adeyeye, A. O.; Welland, M. E. Sensing magnetic fields using superparamagnetic nanomagnets. J. Appl. Phys. **2000**, *87*(9), 7082–7084.
22. Iglesias, O.; Labarta, A. Finite-size and surface effects in maghemite nanoparticles: Monte Carlo simulations. Phys. Rev. B **2001**, *63*(18), 184416.
23. Ben Youssef, J.; Brosseau, C. Magnetization damping in two-component metal oxide micropowder and nanopowder compacts by broadband ferromagnetic resonance measurements. Phys. Rev. B **2006**, *74*(21), 214413.
24. Bødker, F.; Mørup, S.; Linderoth, S. Surface effects in metallic iron nanoparticles. Phys. Rev. Lett. **1994**, *72*(2), 282–285.
25. Spinu, L.; O'Connor, J.; Srikanth, H. Radio frequency probe studies of magnetic nanostructures. IEEE Trans. Magnetism **2001**, *37*(4), 2188–2193.
26. Mallegol, S.; Brosseau, C.; Queffelec, P.; Konn, A.-M. Measurement of the permeability tensor in nanophases of granular metal oxides and field-induced magnetic anisotropy. Phys. Rev. B **2003**, *68*(17), 174422.

27. Brosseau, C.; Mallegol, S.; Queffelec, P.; Ben Youssef, J. Nonreciprocal electromagnetic properties of nanocomposites at microwave frequencies. Phys. Rev. B **2004**, *70*(9), 092401.
28. Queffelec, P.; Mallegol, S.; Le Floc'h, M. Automatic measurement of complex tensorial permeability of magnetized materials in a wide microwave frequency range. IEEE Trans. Microwave Theory Techniques **2002**, *50*(9), 2128–2134.
29. Brosseau, C.; Beroual, A. Computational electromagnetics and the rational design of dielectric heterostructures. Prog. Mater. Sci. **2003**, *48*(5), 373–456.
30. Viau, G.; Ravel, F.; Acher, O.; Fiévet-Vincent, F.; Fiévet, F. Preparation and microwave characterization of spherical and monodisperse Co-Ni particles. J. Magnetism Magnetic Mater. **1995**, *140–144*(1), 377–378.
31. Brosseau, C.; Ben-Youssef, J.; Talbot, P.; Konn, A.-M. Electromagnetic and magnetic properties of multicomponent metal oxides heterostructures: nanometer versus micrometer-sized particles. J. Appl. Phys. **2003**, *93*(11), 9243–9256.
32. Brosseau, C.; Talbot, P. Effective magnetic permeability of Ni and Co micro- and nanoparticles embedded in a ZnO matrix. J. Appl. Phys. **2003**, *97*(10), 104325–104335.
33. Nicolson, A. M.; Ross, G. F. The measurement of intrinsic properties of materials by time domain techniques. IEEE Trans. Instrumentation Measurement **1970**, *19*(11), 377–383.
34. Hill, N. A. Why are there so few magnetic ferroelectrics? J. Phys. Chem. B **2000**, *104*(29), 6694–6709.
35. Brosseau, C.; Talbot, P. Effective permittivity of nanocomposite powder compacts. IEEE Trans. Dielectrics Electrical Insulation **2004**, *11*(3), 819–832.
36. Mercier, D.; Levy, J. C. S.; Viau, G.; Fiévet-Vincent, F.; Fiévet, F.; Toneguzzo, P.; Acher, O. Magnetic resonance in spherical Co-Ni and Fe-Co-Ni particles. Phys. Rev. B **2000**, *62*(1), 532–544.
37. The term magnetoelectric is reserved for the special symmetries where a free energy invariant proportional to P.M is allowed, where *P* and *M* denote the polarization and the magnetization, respectively, see Landau, L. D.; Lifshitz, E. M.; Pitaevskii, L. D. *Electrodynamics of Continuous Media*; Pergamon: New York, 1984; 476.
38. Zheng, H.; Wang, J.; Lofland, S. E.; Ma, Z.; Mohaddes-Ardabili, L.; Zhao, T.; Salamanca-Riba, L.; Shinde, S. R.; Ogale, S. B.; Bai, F.; Viehland, D.; Jia, Y.; Schlom, D. G.; Wuttig, M.; Roytburd, A.; Ramesh, R. Multiferroic $BaTiO_3$-$CoFe_2O_4$ Nanostructures. Science **2004**, *303*(5658), 661–663.
39. Freeman, A. J.; Schmid, H.; Eds. *Magnetoelectric Interaction Phenomena in Crystals*; Gordon and Breach: London, 1975; 1–228.
40. Moreira dos Santos, A.; Parashar, S.; Raju, A. R.; Zhao, Y. S.; Cheetham, A. K.; Rao, C. N. R. Evidence for the likely occurrence of magnetoferroelectricity in the simple perovskite, $BiMnO_3$. Solid State Commun. **2002**, *122*(1–2), 49–52.